

Free Volume in Polyimides: Positron Annihilation Experiments and Molecular Modeling

J. Kruse,[†] J. Kanzow,[†] K. Rätzke,[†] F. Faupel,^{*,†} M. Heuchel,[‡] J. Frahn,[‡] and D. Hofmann[‡]

Lehrstuhl für Materialverbunde, Technische Fakultät der Christian-Albrechts-Universität zu Kiel, Kaiserstrasse 2, 24143 Kiel, Germany, and GKSS Forschungszentrum GmbH, Institut für Chemie, Kantstrasse 55, D-14513 Teltow, Germany

Received December 22, 2004; Revised Manuscript Received August 24, 2005

ABSTRACT: We present a combined analysis of the free volume in polyimide membrane polymers by employing experimental measurements as well as computer simulations. The amount and distribution of free volume in polymeric membranes significantly determine the transport and separation properties. In the present work these free volume characteristics were determined directly from simulated atomistic packing models via a new method. Here a “virtual tracer sphere” probes the simulation cell to determine the unoccupied volume. As an experimental approach, positron annihilation lifetime spectroscopy was used to determine the average size of free volume cavities via a well-established correlation between orthopositronium lifetime and cavity size. We show that the results obtained from the combined analysis provide a valuable basis for the investigation of free volume properties; moreover, limitations of the standard model for the evolution of the positron lifetime data will be discussed.

Introduction

Membranes for separation of gases and vapors are increasingly investigated and applied for many technical applications. Examples can be found in the recovery of process gases in the chemical industry. In particular, glassy polymers are used due to the ease of production, modification, and operation at low temperatures. Special care has to be taken to create polymers with a high free volume as the free volume in glassy polymers is widely accepted as a crucial factor affecting efficiency of membrane applications.^{1–3} One common class of membrane polymers are aromatic polyimides,⁴ where the rigid backbone gives rise to a high free volume fraction. Conversely, conventional polymers like polystyrene and polypropylene are not perfectly suited due to their low free volume fraction. Good correlation between free volume and diffusivities of gas molecules has been reported.⁵ At a first glance, the free volume can be easily calculated as the difference between the overall volume and the volume occupied by molecular segments (Bondi method⁶) or experimentally determined from positron lifetime in connection with pressure–volume–temperature (PVT) experiments.⁷ However, for membrane applications, only that part of the free volume is important which is accessible to the diffusing species. Thus, the accessible free volume will be the object of this investigation.

A common experimental approach to determine the free volume in polymers is given by the positron annihilation lifetime spectroscopy (PALS). Positrons obtained from radioactive decay annihilate with electrons in the polymer material. Some of the positrons and electrons form a hydrogen atom like state called positronium inside free volume cavities in the polymer. If the spins of electron and positron add to a value of

one, annihilation of this orthopositronium (o-Ps) is impeded, reducing the decay rate drastically. Now the interaction of the o-Ps with the electrons in the surrounding material will be the reason for annihilation because an exchange of the electrons can change the state of the orthopositronium into the fast decaying para-state. Thus, the local electron density, which is lower in larger holes, becomes a measure for the hole size.

The average decay rate of orthopositronium in the polymer is measured and correlated to the average size of the microvoids via a well-established semiempirical equation.^{8–10} Assuming the positronium to be confined in a spherical potential well of infinite wall height, the Schrödinger equation for the particle can be formulated and solved analytically. Integration of the probability density function in an electron layer of fixed annihilation rate and experimentally calibrated width yields the relation between hole radius and positronium lifetime:

$$\tau_{o-Ps} = \lambda_0^{-1} \left(1 - \frac{R_h}{R_h + \delta R} + \frac{1}{2\pi} \sin\left(\frac{2\pi R_h}{R_h + \delta R}\right) \right)^{-1} \quad (1)$$

where τ_{o-Ps} denotes the reciprocal orthopositronium decay rate, λ_0 the spin-averaged decay rate, R_h the hole radius, and δR the thickness of the electron layer.

This average free volume has frequently been used to characterize membrane properties.^{11–13} However, the main problem is that it does not give any insight into size distributions of free volume which is the objective of the present investigation.

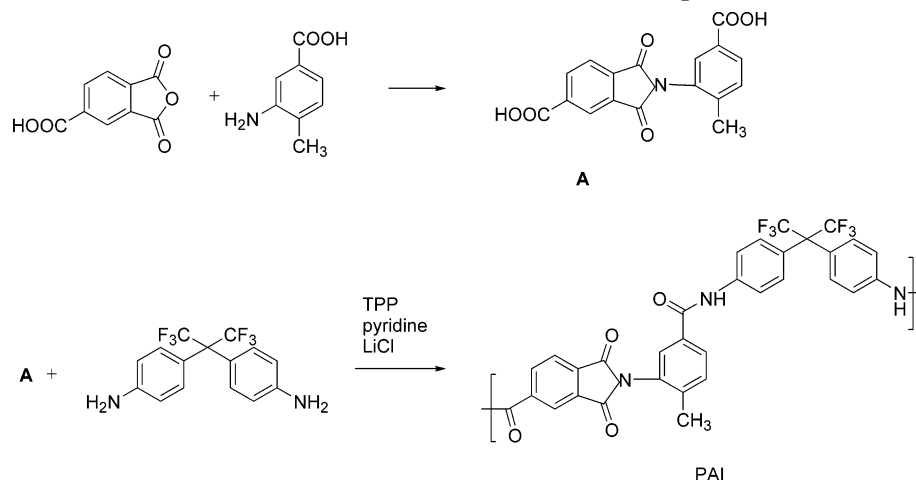
On the other hand, increasing computation power allows detailed and accurate molecular modeling of polymer structures consisting of several thousand atoms. Hence, it is now possible to make well-equilibrated packing models for glassy polymer structures.¹⁴ We have developed a new method¹⁵ to evaluate the accessible free volume by probing the simulation cell with a “virtual tracer sphere” in order to obtain insight into hole size

[†] Technische Fakultät der Christian-Albrechts-Universität zu Kiel.

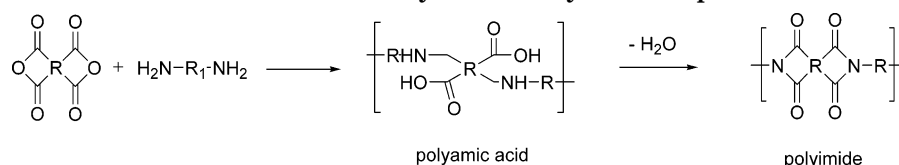
[‡] Institut für Chemie, GKSS Teltow.

* Corresponding author. E-mail: ff@tf.uni-kiel.de.

Scheme 1. Reaction Scheme for the PAI Preparation



Scheme 2. Schematic Way for the Polyimide Preparation



distribution, concentration, shape, and total volume fraction of accessible free volume.

In this paper, we will combine these two methods by applying them to aromatic polyimides with a high glass transition temperature $\sim 350^\circ\text{C}$ and a high free volume; some formed by including the 6FDA group (hexafluoroisopropane dianhydride), which is a promising candidate to membrane applications due to the rigid hindrance of close polymer chain packing¹⁶ (see above). Although various polyimides are known to be strong positronium inhibitors, this does apparently not apply to the 6FDA-based polyimides.¹⁷ We will show results indicating the good correlation of free volume determined from these two very different methods, and we will discuss the suitability of the combination to comparison with transport mechanisms in polymer membranes.

Experimental Section

Sample Preparation. The poly(amide imide) PAI was synthesized by direct polycondensation of dicarboxylic acid **A** (see Scheme 1) with diamine (6FDANH₂) following the Yamazaki route which was developed originally for polyamide.¹⁸ The dicarboxylic acid **A** including the imide structure was synthesized reacting 1,2,4-benzenetricarboxylic anhydride (trimellitic anhydride) with 3-amino-4-methylbenzoic acid. This procedure for the PAI preparation with triphenyl phosphite (TPP), pyridine, and LiCl as reagents was described by Fritsch and Peinemann.^{19–21} Homogeneous, pore-free films were prepared from *N*-methyl-2-pyrrolidone (NMP) solutions. Residual solvent was removed by solvent exchange with methanol and drying to constant weight in a vacuum oven at 120°C .

The polyimides BAAF and PI4 were prepared by a two-step method.^{22,23} First, a polyamic acid was synthesized by adding solid 2,2'-bis(3,4-dicarboxyphenyl)hexafluoropropane dianhydride (6FDA) to a solution of recrystallized diamine (Scheme 2) in freshly distilled NMP. The dianhydride-to-diamine molar ratio was maintained at 1:1. The reaction mixture was stirred for at least 20 h at room temperature to form a highly viscous polyamic acid/NMP solution. Then it was imidized to form polyimide. The cyclization was achieved by chemical imidization through the addition of a weak base (triethylamine) and a dehydrating agent (acetic anhydride) into the polyamic acid solution and then reacted for 3 h at 50°C .

The polymers were recovered by precipitation twice in methanol, followed by an intensive washing with methanol and deionized water. The polymers were dried overnight at 150°C in a vacuum oven. Homogeneous, pore-free films were prepared from NMP solutions. The filtered solution was casted onto a glass plate using a surgical knife and dried at 80°C for 12 h. The polyimide films were removed from the glass plate with water, dried at 80°C , and then finally dried in oil pump vacuum at 150°C for at least 48 h.

Table 2 contains, next to names for the polymers used in other experimental investigations, the density of the samples and the observed glass transition temperature detected by either differential scanning calorimetry (DSC) or dynamical mechanical thermal analysis (DMTA). The molecular weights were determined by GPC. The mobile phase was CHCl_3 for PI4 and THF for BAAF and PAI. M_n and M_w were calculated from universal calibration curves obtained from polystyrene standards. As an example for the gas transport properties of the investigated material, also the solubility coefficient and diffusion coefficient of oxygen are presented which were determined by time-lag experiments at 30°C and 1 bar feed pressure. Further physical properties of the investigated polymers may be found in the literature, e.g., for PAI,²⁴ BAAF,²⁵ and for PI4.²⁶

Positron Annihilation. Before measuring, all films were rinsed with methanol to remove surface contamination. Subsequently, all samples were annealed in high vacuum at 100°C for >24 h. For measurements, the temperature was set to 30°C to allow future comparison with permeation measurements. The pressure was kept below 10^{-6} mbar to avoid occupation of cavities by gas molecules and annihilation in air. PALS measurements were performed using a fast-fast coincidence setup.²⁴ As a positron source, radioactive ^{22}Na (in the form of NaCl, in aqueous solution) was applied between two film cuts of $9 \times 9 \text{ mm}^2$ to obtain a so-called sandwich geometry. To meet the penetration depth of positrons emitted by ^{22}Na , film samples were stacked to a resulting thickness of 1 mm each side, typically 10 pieces of $100 \mu\text{m}$ on each side. Because of this and the high-vacuum conditions surface contributions and contributions from annihilation in air could be neglected. Almost simultaneous to the emission of a positron from the decaying ^{22}Na , a 1.28 MeV γ -quantum is emitted, serving as a "start" signal for lifetime measurement. The "stop" signal is given by one of the two 511 keV γ -quanta emitted from positron annihilation. A multichannel analyzer recorded spec-

Table 1. Polyimide Structures and Their Building Blocks

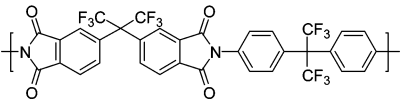
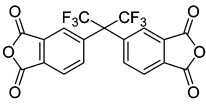
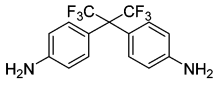
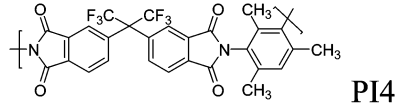
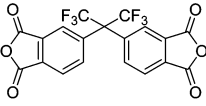
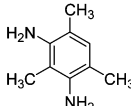
Polymer	Dianhydride component	Diamine component
 <p style="text-align: center;">BAAF</p>		
 <p style="text-align: center;">PI4</p>		

Table 2. Physical Properties of the Investigated Polymers

polymer	name	density (g/cm ³)	<i>T</i> _g (°C)	<i>M</i> _w (kg/mol)	<i>M</i> _w / <i>M</i> _n	<i>S</i> _{O₂} (1/bar)	<i>D</i> _{O₂} (10 ⁻⁸ cm ³ /s)
PI4	6FDA-3MPD	1.32	380	316	2.2	2.29	52
BAAF	6FDA-DAM						
	6FDA-BAAF	1.47	303	96	1.3	0.95	10
	6FDA-6FpDA						
PAI		1.39	355 ^a	90	1.8	0.40	3

^a From DMTA (see ref 24).

tra consisting of 8×10^6 of such events for the polyimides and 4×10^6 for poly(amide imide) due to a lower source activity. Spectra analysis was performed with the discrete lifetime analysis routine PATFIT88 similar to previous investigations.²⁴ All spectra were evaluated with three discrete lifetime components, of which the third one τ_3 is assigned to the decay of orthopositronium. The lower lifetime components originate from decay processes not directly related to free volume size and will not be discussed here.

In general, polyimides are known to strongly suppress positronium formation (Ps inhibition). The model system PMDA-ODA (Kapton) shows no significant long lifetime component, although the aromatic backbone structure should provide sufficiently large free volume holes for accommodation of positronium. However, this inhibition effect seems to be not specific to all polyimides but mainly depends on the chemistry of the dianhydride.²⁷ Okamoto et al. have demonstrated that the inhibition and quenching effect of the 6FDA seems to be negligible. The occurrence of a pronounced long lifetime component in our measurements is in good accordance with their observations.

The three-component lifetime analysis gave a small fit error on all investigated polyimides, indicating that no further lifetimes occurred. This was also cross checked by data evaluation with the continuous lifetime distribution analysis routine MELT.²⁸ Discrete lifetimes and maxima in the distribution coincided well. We did also take into account the known difficulties of evaluation with distributions of free volume and hence distribution in τ_3 leading to improper τ_1 values.²⁹ However, a conversion of the width of the lifetime distribution to a width in free volume cavity distributions is not useful due to the simplifications of the conversion (eq 1) and the weighting factor of the large cavities for lifetimes (see below). Table 3 lists the values of the orthopositronium lifetimes of the three polyimides under investigation. The hole radii calculated with eq 1 are listed in Table 3.

The order of magnitude of the positronium lifetimes is the expected one for high free volume membrane polymers and for polyimides in particular, as comparison with literature shows.^{13,24}

Molecular Modeling

Details of Modeling. Amorphous packing models were constructed and simulated for the three polymers

Table 3. Orthopositronium Lifetimes and Calculated Hole Radii from Eq 1^a

polymer	τ_{o-Ps}	hole radius
PI4	3.7 ns \pm 10 ps	0.4075 nm \pm 0.6 pm
BAAF	3.23 ns \pm 17 ps	0.3788 nm \pm 1.0 pm
PAI	2.82 ns \pm 103 ps	0.3513 nm \pm 7.2 pm

^a In place of errors, the standard deviation from PATFIT results are given. The higher deviation value of PAI can be explained with the lower count number and a lower signal intensity.

by means of the InsightII/Discover software of Accelrys Inc.³⁰ The general approach for the atomistic packing model construction is described in ref 31. The basis for the calculation is the force field, i.e., the summarized parameter set describing energy contributions from bond length, bond angles, conformation angles, and the nonbond interactions. For PAI first the cvff force field^{32,33} was chosen and later, as for the polyimides PI4 and BAAF, the more recent COMPASS force field^{34,35} of Accelrys. The calculations have been performed on two SGI Octane machines and an 8-processor SGI 2100.

The principal course of the packing algorithm for a polymer was as follows: In a first stage a repeat unit was built. The polymer chains were constructed using the polymerizer module³⁶ of the Accelrys software. The chains were then subjected to a static structural optimization via a steepest decent energy minimization. The resulting objects served as topological templates for an initial guess filling of periodic boxes with chain segments. It should be mentioned that by using periodic boundary conditions, finally all segments are continued over the limits of the basic volume cell as part of copies of the originally grown chain. For this initial packing procedure the Theodorou-Suter approach^{37,38} was used. The polymer chains were packed at 300 K under cubic periodic boundary conditions. The volume of the basic cell was chosen that a very low initial packing density of typically 0.1 g/cm³ was obtained. This helped already to avoid artifacts of catenated phenylene rings or spearing of side groups through ring substructures

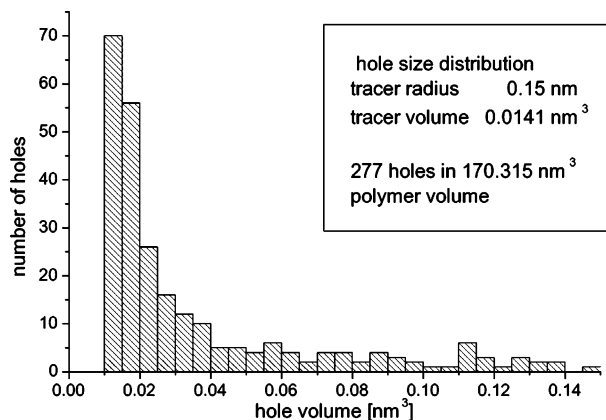


Figure 1. Hole size distribution in BAAF for tracer radius 0.15 nm, up to 0.150 nm³.

which may appear. Additionally during the initial packing a set of small molecules have been added as randomly distributed obstacles, preventing the respective growing polymer chains from ring catenations and spearings. Details of these approach for the polyimides are summarized in ref 14.

All initial packing models consisting of about 4500 atoms (60–80 repeat units) had then to be subjected to extensive equilibration procedures (see also ref 14) containing (1) energy minimization and MD runs combined with “scaling” of conformation energy terms and nonbonded interaction energy terms in the force field, (2) sets of MD runs to increase the density, and (3) longer MD runs for the final equilibration.

At least three independent packing models were build for every polymer. These models correspond to three different possible local chain segment assemblies of the respective polymer. The quality of the final packing models was validated at first by stable density fluctuations around the experimental density during longer (at least 300 ps) MD runs at constant pressure of $P = 1$ bar. A further check was the calculation of gas transport data for small gases on the basis of these packing models. For nitrogen and oxygen, both gas solubility and diffusion coefficient have been determined with the Gusev–Suter transition state theory.³⁹ Good agreement with experiment (factor 1–4) was found. The respective calculations are described for PI4 and BAAF in ref 14 and for PAI in ref 40.

Evaluation of the Modeling Data. The evaluation of the simulation results is based on a three-dimensional raster with a mesh width of 5 pm. By attributing atomic van der Waals radii to the atom positions in the results data, certain areas in the raster cell can be marked as occupied by atoms.¹⁵

To probe the “accessible” free volume, we used a “tracer” sphere of radius 0.15 nm, which is the size of small gas molecules, and tested the whole MD cell, whether this atom fits into unoccupied space and how large the corresponding hole is. However, the “accessible free volume” can be significantly smaller than the unoccupied volume fraction, and its properties depend on the tracer radius.

In the simulation cells investigated in this work, up to several hundred isolated (separated) holes were detected. The resulting lists of holes were then analyzed with respect to size, number, and shape, so that information about hole density and size distribution is available. Figure 1 shows a typical hole size distribution

for the polyimide BAAF as detected with a tracer of radius 0.15 nm.

Obviously, larger holes occur with a lower probability than small holes, and the occurrence decreases monotonically with the hole volume, showing no concentration of holes in any certain volume interval. Simple averaging over the data in Figure 1 gives a mean value of 0.0584 nm³ (number-average); however, this value will not be useful with respect to further evaluations. Weighted averages will be discussed in connection with comparison to positronium lifetime.

Another information which can be derived from this is the absolute amount of free volume in the simulation cell. We have a number of holes of given size or size interval, and we have their respective volume. From this we can calculate the absolute value of fractional free volume for the respective tracer size. As the size of the simulation cell is known, we can easily calculate the fractional free volume by dividing the absolute amount of free volume of all cavities by the volume of the cell. Fractional free volume ranges from 7% to 10% for a tracer sphere of 0.15 nm radius, which is in good accordance with literature values.⁴¹ The same holds for the hole concentration, which can be calculated by counting the absolute number of holes in the simulation cells and dividing this value by the respective cell volume. Typical values of 10²¹ cm⁻³ are obtained from this method.

Comparison of the Two Methods

In the following, a comparison between the average free volume size as resolved by the positron annihilation and the free volume, as determined from the MD simulation will be made. To the authors knowledge, there is only one attempt⁴² to directly calculate the positron lifetime for each volume element of a MD cell. Although done with great care, even for simple polystyrene a difference of a factor of 3 between experiment and calculation remains due to uncertainties in modeling the positron decay process.⁴² Hence, for the present, much more complex polyimides we did not use this model but restricted ourselves to comparison of suitable averaged values.

As already mentioned in the previous paragraph, a simple averaging over the number of the free volume holes is not useful because the small holes do not contribute significantly to the membrane and transport properties; hence, a weighting step will be necessary. Up to this point, the relative contribution of the hole size to the total amount of free volume is not included. Therefore, the hole volume itself is introduced as a weighting factor, so that a large number of small holes will have the same weight as small amount of large holes. The modified graph in Figure 2 shows the distribution of the accessible free volume with respect to the hole size.

As a measure for comparing the weighted hole numbers with experimental data, a new “mean value” V50 was defined in analogy to a median value. V50 splits the total available volume into two halves; i.e., 50% of the available free volume is smaller than this value (please note: this does not mean that 50% of the holes are smaller; the hole volume is included in the calculation as a weighting factor). If all holes would be spheres and equally be probed by the positronium, the average volume from positron lifetime should be equal to this V50.

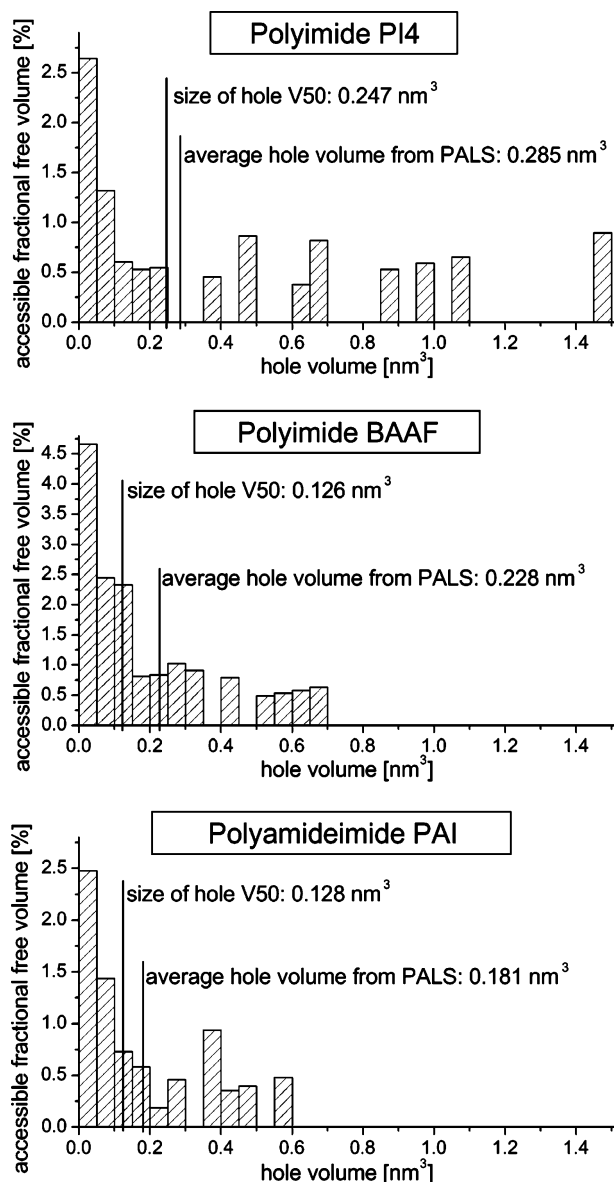


Figure 2. Weighted distribution of hole volume and average values (for details see text).

Table 4. Comparison of Free Volume from Positron Annihilation Data (V_{PALS}) and from MD Simulations (V50, Accessible Fractional Free Volume)

polymer	V_{PALS} (nm ³)	V50 (nm ³)	V50 (nm ³)	ffv (%)
PI4	0.2835 ± 0.00115	0.244 15	0.247	9.8 ± 0.22
		0.398 69		
		0.247 26		
BAAF	0.2278 ± 0.00115	0.125 57	0.126	8.75 ± 0.3
		0.134 79		
		0.119 96		
PAI	0.1817 ± 0.00653	0.089 87	0.128	7.27 ± 0.3
		0.170 76		

The corresponding values are summarized in Table 4. The error in V_{PALS} is derived from the error in the positron lifetime. Concerning V50, we evaluated up to three different MD cells and give all results in Table 4, third column. Simple averaging is feasible, but as a closer inspection of data and corresponding MD cells shows, some cells show exceptionally high values of free volume, agglomerated into one big, jagged hole. We assume that this is an artifact due to the small size of the MD cell. Therefore, it is useful to neglect these values while averaging, and the corresponding reason-

able mean values are plotted in Figure 2 and listed in Table 4, fourth column. The agreement is generally good, and in particular the tendency comparing the different polyimides is good. However, the average free volume as determined by positron annihilation is always larger than the V50. Possible explanations for this are discussed in the following.

Although it is known that larger holes are not spherical,¹⁵ this cannot explain the deviation discussed above because for a given volume the lifetime inside the sphere is always the largest one.⁴³ Hence, for a measured lifetime the volume of the sphere attributed via eq 1 is always the smallest one possible.

When the “virtual tracer sphere” is used to probe a simulation cell, the sphere radius becomes a crucial factor. Although positronium and hydrogen atom have the same size in Bohr’s model, this can obviously not be transferred to the van der Waals radius of the positronium. The details of tracer size effects will be treated in a following paper.

The most important deviation might be attributed to the tendency of the positronium to probe several holes after formation, as the positronium diffusion length is of the order of 15 nm.⁴⁴ Moreover, the trapping probability is not known and might depend on the size of the respective hole.

Therefore, the main reasons for the remaining deviation can be attributed to the details of the interaction of the positronium with the sample and will be included in a more detailed analysis.

In conclusion, it has been shown that free volume, which is a key quantity for polymeric membranes, can be determined by positron annihilation, and the quantities are in good accordance with results from evaluation of MD simulations.

Acknowledgment. The authors thank Prof. Dr. G. Dlubek, Halle for helpful discussions. Financial support of this project by GKSS Hochschulprogramm is gratefully acknowledged.

References and Notes

- (1) Paul, D. R.; Yampolskii, Yu. P. *Polymeric Gas Separation Membranes*; CRC Press: Boca Raton, FL, 1994.
- (2) Robeson, L. M.; Burgoyne, W. F.; Langsam, M.; Savoca, A. C.; Tien, C. F. *Polymer* **1994**, *35*, 4970–4978.
- (3) Langsam, M. In *Polyimides: Fundamentals and Applications*; Ghosh, M. K., Mittal, K. L., Eds.; Marcel Dekker: New York, 1996.
- (4) Pixton, M. R.; Paul, D. R. In *Polymeric Gas Separation Membranes*; Paul, D. R., Yampolskii, Yu. P., Eds.; CRC Press: Boca Raton, FL, 1994.
- (5) Nagel, C.; Günther-Schade, K.; Fritsch, D.; Strunskus, T.; Faupel, F. *Macromolecules* **2002**, *35*, 2071–2077.
- (6) Bondi, A. *Physical Properties of Molecular Crystals, Liquids, and Glasses*; Wiley: New York, 1968.
- (7) Dlubek, G.; Wawryszczuk, J.; Pionteck, J.; Goworek, T.; Kaspar, H.; Lochhaas, K. H. *Macromolecules* **2005**, *38*, 429–437.
- (8) Tao, S. J. *J. Chem. Phys.* **1972**, *56*, 5499–5510.
- (9) Eldrup, M.; Lightbody, D.; Sherwood, J. N. *Chem. Phys.* **1981**, *63*, 51–58.
- (10) Jean, Y. C. *Microchem. J.* **1990**, *42*, 72–102.
- (11) Alentiev, A.; Shantarovich, V.; Merkel, T.; Bondar, V.; Freeman, B.; Yampolskii, Y. *Macromolecules* **2002**, *35*, 9513–9522.
- (12) Ronova, I.; Yampolskii, Y. *Macromol. Theory Simul.* **2003**, *12*, 425–439.
- (13) Jean, Y.; Mallon, P.; Schrader, D. *Positron and Positronium Chemistry*; World Scientific: Singapore, 2003.
- (14) Heuchel, M.; Hofmann, D.; Pullumbi, P. *Macromolecules* **2004**, *37*, 201–214.

- (15) Schmidtke, E.; Günther-Schade, K.; Hofmann, D.; Faupel, F. *J. Mol. Graphics Modell.* **2004**, *22*, 309–316.
- (16) Heuchel, M.; Hofmann, D. *Desalination* **2002**, *144*, 67–72.
- (17) Ito, Y. *Mater. Sci. Forum* **1995**, *175–178*, 627–634.
- (18) Yamazaki, N.; Matsumoto, M.; Higashi, F. *J. Polym. Sci., Part A: Polym. Chem.* **1975**, *13*, 1373–1380.
- (19) Fritsch, D.; Peinemann, K.-V. *J. Membr. Sci.* **1996**, *99*, 29–38.
- (20) Fritsch, D.; Avella, N. *Macromol. Chem. Phys.* **1996**, *197*, 701–714.
- (21) Fritsch, D.; Peinemann, K.-V.; Behling, R. D. DE-OS Pat. 42 62 496 A1, 1994.
- (22) Lin, W.-H.; Vora, R. H.; Chung, T.-S. *J. Polym. Sci., Part: B Polym. Phys.* **2000**, *38*, 2703–2713.
- (23) Tanaka, K.; Okano, M.; Toshino, H.; Kita, H.; Okamoto, K. *J. Polym. Sci., Part B: Polym. Phys.* **1992**, *30*, 907–914.
- (24) Nagel, C.; Schmidtke, E.; Günther-Schade, K.; Hofmann, D.; Fritsch, D.; Strunskus, T.; Faupel, F. *Macromolecules* **2000**, *33*, 2242–2248.
- (25) Costello, L. M.; Koros, W. J. *J. Polym. Sci., Part B: Polym. Phys.* **1995**, *33*, 135–136.
- (26) Yeom, C. K.; Lee, J. M.; Hong, Y. T.; Choi, K. Y.; Kim, S. C. *J. Membr. Sci.* **2000**, *166*, 71–83.
- (27) Okamoto, K.-I.; Tanaka, K.; Katsube, M.; Sueoka, O.; Ito, Y. *Radiat. Phys. Chem.* **1993**, *41*, 497–502.
- (28) Shukla, A.; Peter, M.; Hoffmann, L. *Nucl. Instrum. Methods A* **1993**, *335*, 310–317.
- (29) Dlubek, G.; Eichler, S.; Hübner, C.; Nagel, C. *Phys. Status Solidi A* **1999**, *174*, 313–325.
- (30) *Polymer User Guide, Amorphous Cell Section*, Version 4.0.0; Molecular Simulations: San Diego, 1996.
- (31) Hofmann, D.; Fritz, L.; Ulbrich, J.; Schepers, C.; Böhning, M. *Macromol. Theory Simul.* **2000**, *9*, 293–327.
- (32) Hagler, A. T.; Lifson, S.; Dauber, P. *J. Am. Chem. Soc.* **1979**, *101*, 5122–5130.
- (33) Hagler, A. T.; Lifson, S.; Dauber, P. *J. Am. Chem. Soc.* **1979**, *101*, 5131–5141.
- (34) Sun, H.; Rigby, D. *Spectrochim. Acta* **1997**, *53A*, 1301–1323.
- (35) Rigby, D.; Sun, H.; Eichinger, B. E. *Polym. Int.* **1997**, *44*, 311–330.
- (36) *Polymer User Guide, Polymerizer Section*, Version 4.0.0; Molecular Simulations: San Diego, 1996.
- (37) Theodorou, D. N.; Suter, U. W. *Macromolecules* **1985**, *18*, 1467–1478.
- (38) Theodorou, D. N.; Suter, U. W. *Macromolecules* **1986**, *19*, 139–154.
- (39) Gusev, A. A.; Suter, U. W. *J. Chem. Phys.* **1993**, *99*, 2228–2234.
- (40) Hofmann, D.; Fritz, L.; Ulbrich, J.; Paul, D. *Polymer* **1997**, *38*, 6145–6155.
- (41) Bohlen, J.; Kirchheim, R. *Macromolecules* **2001**, *34*, 4210–4215.
- (42) Schmitz, H.; Müller-Plathe, F. *J. Chem. Phys.* **2000**, *112*, 1040–1045.
- (43) Goworek, T. *J. Nucl. Radiochem. Sci.* **2000**, *1*, 11–13.
- (44) Cao, H.; Zhang, R.; Yuan, J.-P.; Huang, C.-M.; Jean, Y. C.; Suzuki, R.; Ohdaira, T.; Nielsen, B. *J. Physics: Condens. Matter* **1998**, *10*, 10429–10442.

MA0473521